

Design of “Smart” flap actuators for swept shock wave/turbulent boundary layer interaction control

Jonathan Couldrick[†], Krishnakumar Shankar[‡], Sudhir Gai^{‡†} and John Milthorpe[‡]

*School of Aerospace & Mechanical Engineering, University College, UNSW,
Australian Defence Force Academy, Canberra, ACT 2600, Australia*

(Received October 4, 2002, Accepted September 24, 2003)

Abstract. Piezoelectric actuators have long been recognised for use in aerospace structures for control of structural shape. This paper looks at active control of the swept shock wave/turbulent boundary layer interaction using smart flap actuators. The actuators are manufactured by bonding piezoelectric material to an inert substrate to control the bleed/suction rate through a plenum chamber. The cavity provides communication of signals across the shock, allowing rapid thickening of the boundary layer approaching the shock, which splits into a series of weaker shocks forming a lambda shock foot, reducing wave drag. Active control allows optimum control of the interaction, as it would be capable of positioning the control region around the original shock position and unimorph tip deflection, hence mass transfer rates. The actuators are modelled using classical composite material mechanics theory, as well as a finite element-modelling program (ANSYS 5.7).

Key words: piezoelectric material; finite element modelling, design, smart structures technology; shock wave/boundary layer interaction.

1. Introduction

For shock waves, with an upstream Mach number above 1.3, incipient separation occurs and the shock wave foot bifurcates above the boundary layer to form a lambda (λ) foot. The leading shock is usually highly oblique with the trailing part of the lambda foot nearly normal.

Previous work (Kubota and Stollery 1982, Babinsky 1999, Bahi *et al.* 1983, Chen *et al.* 1984, Delery 1985, Delery and Bur 1999, Gibson *et al.* 2000, Nagamatsu *et al.* 1985, 1987, Raghunathan 1987, Raghunathan *et al.* 1987, Raghunathan and Mabey 1987, Raghunathan 1988, Savu and Trifu 1984) has been to passively control the interaction by replacing the surface beneath the foot of the shock wave with a porous plate covering a plenum chamber (Fig. 1). This allows high-pressure air from the flow downstream of the shock wave to re-circulate through the plenum chamber, allowing rapid thickening of the boundary layer approaching the shock, forming a lambda shock foot, reducing wave drag. Furthermore, the suction down-stream reduces separation and viscous losses.

Passive control is shown to be beneficial for freestreams above Mach 1.3. However, at lower

[†] Student

[‡] Doctor

^{‡†} Associate Professor

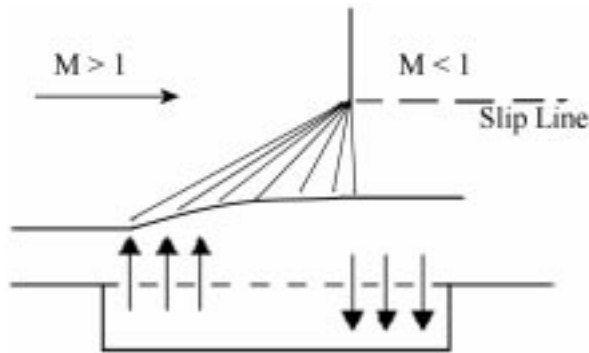


Fig. 1 Passive control of shock/boundary layer interaction (PCSBLI)

freestream velocities the amount of wave drag reduction is offset by the increase in skin friction drag due to the 'rough' control surface, creating an increase in total drag. The amount of wave drag reduction depends on numerous factors that include, shock strength/location (Delery 1985, Delery and Bur 1999, Nagamatsu *et al.* 1985, Raghunathan 1987, Krogmann *et al.* 1985), porosity type/distribution (Bahi *et al.* 1983, Chen *et al.* 1984, Nagamatsu *et al.* 1985, 1987, Raghunathan 1987, Raghunathan *et al.* 1987, Raghunathan and Mabey 1987, Raghunathan 1988) and boundary layer size (Bahi *et al.* 1983).

Historically, active control of shock/boundary layer interaction (ACSBLI) has been hampered by the drag reduction achieved being negated by the additional drag due to the power requirements, for example, the pump in the case of mass transfer and the drag of the devices in the case of vortex generators.

Piezoelectric actuators have long been recognised for use in aerospace structures for control of structural shape (Crawley 1994). The object of the present research is to assess the concept of active control using "smart" flap actuators (Couldrick *et al.* 2001, 2002a, 2002b) (Fig. 2). The actuators (Fig. 3) are designed using PZT-5H piezoelectric material to control bleed/suction rate, whilst retaining a 'smooth' control surface.

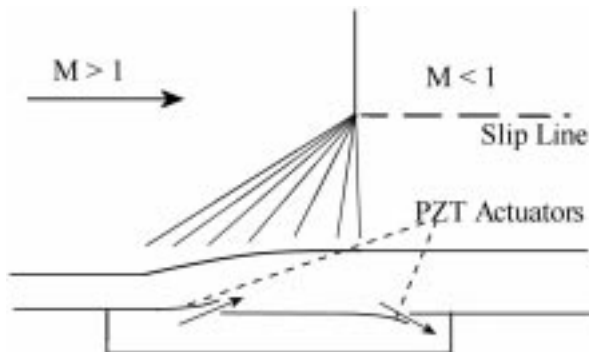


Fig. 2 Active Control of Shock/Boundary Layer Interaction

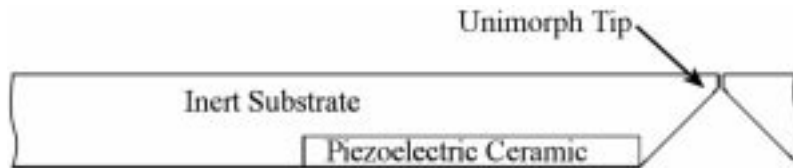


Fig. 3 Modified unimorph flap configuration

2. Experimental arrangement

The experimental work is to be carried out in a blow-down supersonic wind tunnel and a swept shock interaction will be produced on the tunnel sidewall, giving a normal shock Mach number (M_n) of 1.3 with a wedge of 11 degrees mounted on the floor in a Mach 2.0 free stream, (Fig. 4). For a static pressure in the test section of 44 kPa, the smart flaps will then have a 17.64 kPa pressure difference acting across them.

A circular plenum chamber ($\varnothing 140 \text{ mm} \times 20 \text{ mm}$) is placed underneath the swept shock in the sidewall of the test section. This is covered by a plate containing the ‘flaps’ and 47 pressure ports, (Fig. 5). The flaps, which without the piezoelectric ceramic are cantilever beams, are cut into the plate by electro discharge machining (EDM) with a gap of 0.1 mm between the model skin and the flap. The plate is sufficiently anodised to electrically isolate the piezo-ceramic, which is bonded to the underside of the flap, and a voltage is applied to control the actuator deflection and thus mass transfer rate. The surface pressures are recorded using a single transducer which steps through the various ports using a time averaging scanivalve. Surface pressures are recorded in both streamwise and transverse directions.

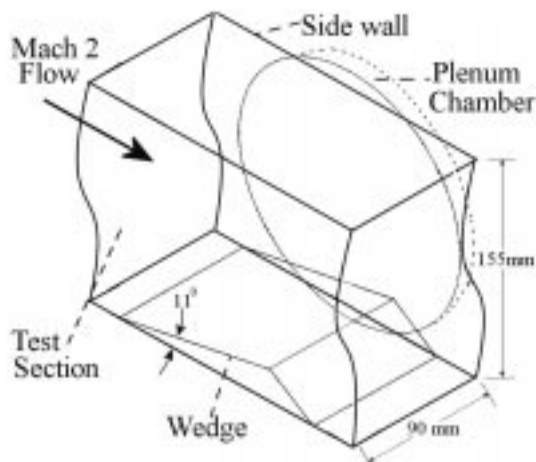


Fig. 4 Experimental arrangement

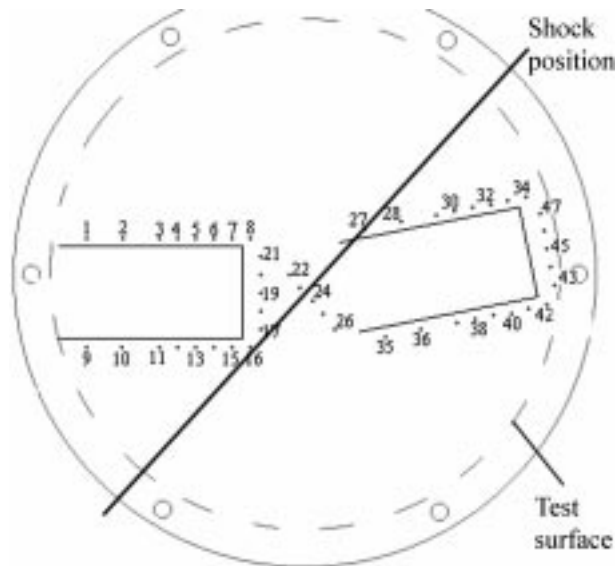


Fig. 5 Generated shock position and pressure port layout on test surface

3. Unimorph actuators

Unimorph tip deflection varies with the substrate's Young's Modulus and thickness (Chattopadhyay and Seeley 1997, Yam and Yan 2002). The selection of substrate is a trade-off between suppressing the pressure deflection whilst keeping the unimorph electrically flexible. Active control of the shock boundary layer interaction requires that the flaps are able to have zero deflection to be regarded as capable of active control. Furthermore, the piezoelectric ceramic will breakdown or depolarise if the mechanical and/or electrical loads exceed their limits, that is too much deflection will degrade the piezoelectric ceramic. It is hoped to achieve improved piezoelectric performance, as a pressure gradient in the plenum chamber and zero pressure loads at the unimorph edge will reduce the pressure difference, from the constant 17.64 kPa, across the unimorphs. For all analyses, the bond/electrode are assumed infinitely thin and stiff. The effects of these and other variables such as temperature and hysteresis are not considered, as this paper concentrates on one design condition with an isotropic and moderately thin composite plate. It is recognised (Chattopadhyay and Seeley 1997, Hwang and Park 1993, Crawley and Luis 1987, Crawley and Lazarus 1991, Matthew *et al.* 2001, Mukherjee and Joshi 2002, Soares *et al.* 1999, Vel and Batra 2000) that further study of these effects would improve results.

4. Determination of tip deflection

4.1 By classical theory

Classical theory (Crawley and Lazarus 1991, Gibson 1994, Donthireddy and Chandrashekhara 1996) uses a combination of composite laminate plate theory (CLPT) and simple beam bending

theory. The effective bending stiffness of the flaps is calculated using CLPT, assuming an infinitely strong bond between the piezoelectric ceramic and substrate. This effective stiffness is then used in classical beam theory to determine the tip deflection of the flap considered as a cantilever beam under various types of pressure loads, namely uniform, linear, etc and due to the induced strain in the PZT layer due to the applied field. For analyses, the piezoelectric strain is assumed to be analogous to a temperature induced strain. The equations of CLPT and the beam theory are implemented using a spreadsheet, giving instantaneous results and it assumes that the total uniform deflection is a summation of the deflections due to the pressure and piezoelectric action.

4.2 Unimorph tip deflection for an applied voltage (δ_V)

Using piezoelectric and laminate theory the deflection obtained when the piezoelectric ceramic has an applied voltage across it, δ_V , is given by,

$$\begin{Bmatrix} \epsilon_i^o \\ \kappa_i \end{Bmatrix} = \begin{bmatrix} A_i & B_i \\ B_i & D_i \end{bmatrix}^{-1} \begin{Bmatrix} N_i \\ M_i \end{Bmatrix} \quad (1)$$

$$\delta_V = \frac{k_i * L^2}{2} \quad (2)$$

In Eq. (1), the extensional stiffness matrix, A_i , relates the induced mid-plane strains, ϵ_i^o , to the induced in-plane forces, N_i , and the bending stiffness matrix, D_i , relates the curvatures, κ_i , to the induced moments, M_i . The coupling stiffness matrix, B_i , couples the induced mid-plane strains, ϵ_i^o , to the induced moments, M_i , and the curvatures, κ_i , to the induced in-plane forces, N_i . L is the length of the unimorph.

The in-plane forces, N , and moments, M , are induced by the voltage applied to the piezoelectric material and can be calculated using,

$$N_{xi} = N_{yi} = \frac{E_P d_{31}}{(1 - \nu_P)} * V \quad (3)$$

$$M_{xi} = M_{yi} = -\frac{E_P d_{31} t_s}{2(1 - \nu_P)} * V = -N_{xi} * \left(\frac{t_s}{2}\right) \quad (4)$$

where E_P , d_{31} , V , ν_P and t_s are the piezoelectric ceramic’s Young’s Modulus, piezoelectric charge constant, applied voltage, piezoelectric ceramic’s Poisson’s ratio and substrate thickness respectively. The load is acting at the centre line of the piezoelectric ceramic, which is at a distance of half the substrate thickness from the laminate centreline.

4.3 Unimorph deflection for a given pressure load (δ_W)

Similarly, laminate theory predicts the unimorph deflection under a given load is given by,

$$\begin{Bmatrix} \epsilon^o \\ \kappa \end{Bmatrix} = \begin{bmatrix} A & B \\ B & D \end{bmatrix}^{-1} \begin{Bmatrix} N \\ M \end{Bmatrix} \quad (5)$$

where N and M are the external applied loads and moments respectively. Then the effective bending stiffness of the composite beam along its length can be obtained as

$$(EI)_{eff} = b/d_{11} \quad (6)$$

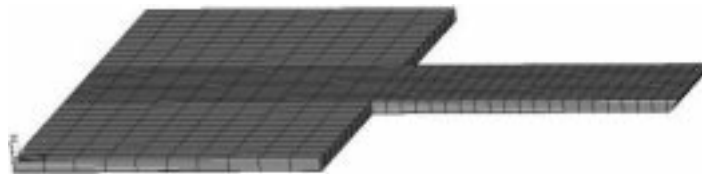
where b is the width of the beam and d_{11} is the first element of the bending element of the flexibility matrix, i.e. the inverse of the laminate stiffness matrix. For any given distribution of pressure loading the tip deflection of the composite cantilever beam can be computed using classical beam theory equations using the effective beam stiffness. For instance, for a constant pressure load P , the tip deflection is given by:

$$\delta_w = PbL^4/8*(EI)_{eff} \quad (7)$$

4.4 By Finite Element Modelling

ANSYS 5.7 was utilised as the FEM program with a parametric design language program to enable the analysis to be repeated simply, quickly and to minimise manual work time. It allowed the parameters to be changed easily and the results recorded as table arrays to minimise memory usage.

The program models the unimorph actuator flap, substrate and piezoelectric ceramic, as well as the supporting substrate structure, (Fig. 6). This could not be performed with the classical theory



(a)

Substrate

Support Structure – 4mm*104mm*52mm

Unimorph – “t” mm*25mm*50mm

Unimorph Tip – (t+0.5) mm*25mm*2mm

Poisson's Ratio $\nu_P = 0.3$

Piezoceramic

Size - 0.5mm*25mm*50mm

Young's Modulus (E_P) – 64 GPa

$d_{31} = -210 * 10^{-12}$ m/V

$d_{33} = 450 * 10^{-12}$ m/V

Poisson's Ratio $\nu_P = 0.45$

(b)

Fig. 6 (a) Unimorph Finite Element Model in ANSYS 5.7, (b) Material characteristics

analysis due to the assumption of a continuous uniform cross section. Furthermore, FEM allows modelling of the solid substrate tip and analysis of complex pressure loadings, which satisfy aerodynamic boundary conditions. On the other hand, the classical theory can only apply simple approximate loads.

The model consists of 3144 Solid95 Brick elements with 1344 elements to model the unimorph. This grid resolution was chosen as a balance between computational cost and sufficient accuracy (Hwang and Park 1993). Zero deflection boundary conditions were placed on all edges of the supporting structure allowing the unimorph flap to freely deflect under the pressure load applied directly to the unimorph flap. FEM only models part of the support structure, as increasing the support structure to the realistic shape does not further improve the results. Furthermore, the improved model would take longer than the 6 hours of computation processing that is required for current analysis for one line on each results graph.

Two design parameters were varied for analysis of the tip deflection. The substrate Young’s Modulus and substrate thickness were varied from 20 GPa to 210 GPa and 0.5 mm to 2.5 mm respectively.

5. Results

5.1 Theoretical deflection variation with substrate thickness for no load

The substrate thickness was altered to observe how the tip deflection would vary using a 500 V applied piezoelectric field (Fig. 7). This analysis used a substrate Young’s Modulus of 70 GPa (aluminium) and the substrate thickness is normalised to the piezoelectric ceramic thickness (X). The results are compared to experimentally obtained data for validation. It is seen that as the substrate thickness increases, the tip deflection increases initially, reaches a peak and then reduces. The theoretical results show good agreement with experimental data.

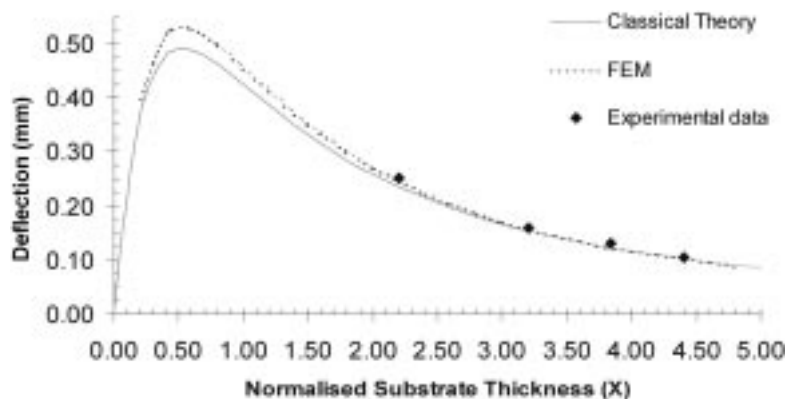


Fig. 7 Unimorph deflection vs. Normalised substrate thickness due to 500 V applied field

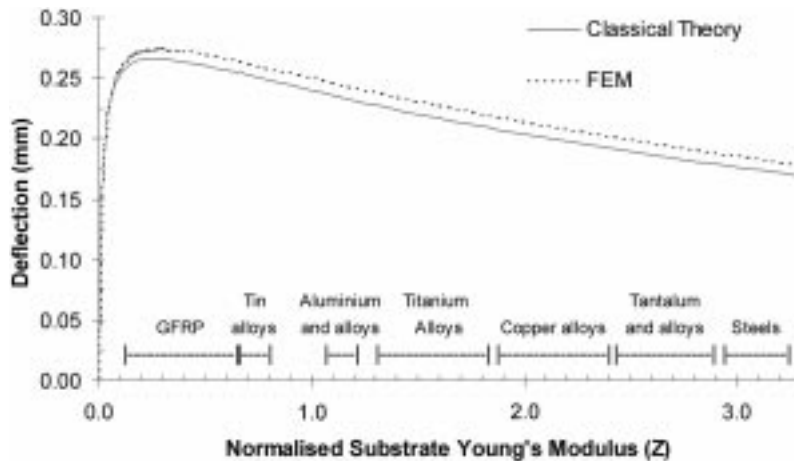


Fig. 8 Deflection vs. Normalised substrate Young's Modulus for 500 V applied field

5.2 Theoretical deflection variation with substrate Young's Modulus for no load

The substrate's Young's Modulus was varied to observe how the tip deflection would vary using a 500 V applied piezoelectric field (Fig. 8). This analysis used a substrate thickness of 1.1 mm ($X = 2.2$) and the substrate's Young's Modulus is normalised to the piezoelectric ceramic's Young's Modulus (Z). A legend of suggested substrate material has been included for the range of Young's Modulus considered.

It is seen that as the substrate thickness or stiffness increases, the tip deflection increases initially, reaches a peak and then reduces. Noting that at zero substrate stiffness there will be no bending deflection as the piezoelectric ceramic is free to expand under the induced strain; as the substrate thickness/stiffness increases from zero, its increasing restraint on the in-plane expansion of the PZT produces an increasing out-of-plane moment causing the composite beam to bend more and more. However as the substrate becomes stiffer due to increasing thickness or increasing Young's Modulus, it becomes more effective in restraining the in-plane expansion of the beam with less deflection, since the applied voltage is unaltered.

The FEM would not allow the substrate's Young's Modulus to go to zero but the two theories show good correlation with each other whilst varying substrate thickness. However, finite element modelling predicts slightly higher tip deflections compared to the classical theory, which is expected to be due to the ability of non-zero deflection characteristics of the support structure not modelled in the classic theory.

5.3 17.64 kPa Constant pressure load predictions

The two modelling systems were tested (Figs. 9a & 9b) to predict the deflection under a uniform pressure load of 17.64 kPa, half the pressure difference between the upstream and downstream pressures. The legend symbols – and + are indicative of negative and positive applied electrical fields respectively. The 0 V trend is approximately the mean of ± 500 V trends and has been omitted from the figures for reasons of overcrowding. Furthermore, no experimental data could be obtained as this

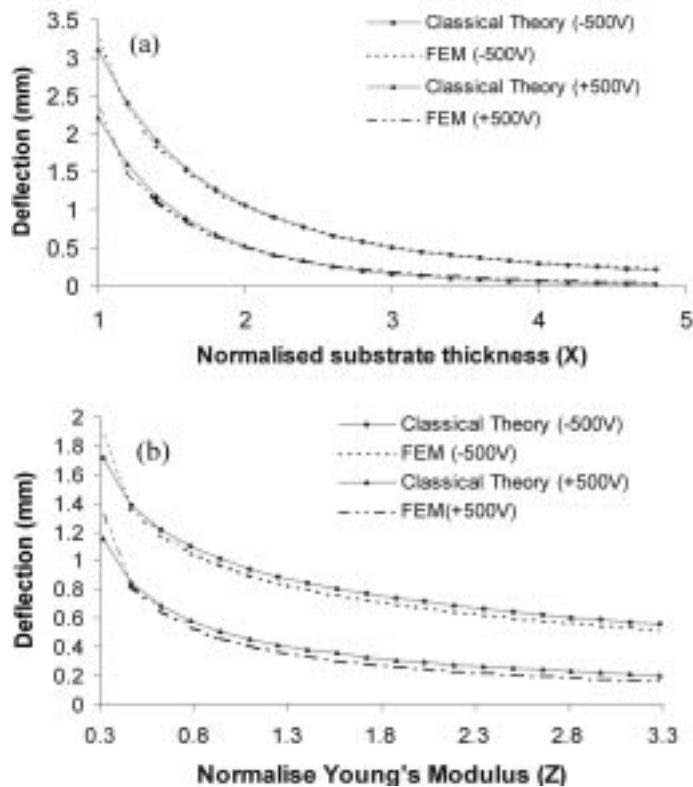


Fig. 9 Tip deflection for a 17.64 kPa uniform pressure load for varying substrate: (a) thickness ($E = 70$ GPa); and (b) Young's Modulus ($t = 1.1$ mm)

is a first order theoretical prediction of the pressure gradient and is hard to physically simulate.

The trend between the classical theory and the finite element results are good for varying both substrate thickness and Young's Modulus. The theoretical results for varying substrate thickness are within 0.1 mm of the finite element modelling. When the normalised substrate thickness is 1.2, deflections of 1.49 and 1.59 mm are predicted for FEM and classic theory respectively.

The theoretical results for varying substrate Young's Modulus are within 0.17 mm of the finite element modelling. When the normalised substrate thickness is 0.3125, deflections of 1.32 and 1.15 mm are predicted for FEM and classic theory respectively. However, after the substrate normalised Young's Modulus is greater than 0.4 the error is reduced to within 0.1 mm.

The differences are suspected to be due to the deviation from perfect built-in condition at the cantilevered end in the FE model, which realistically simulates the support structure around the unimorph allowing non-zero slope at the beginning of the flap.

It is also seen that a 'negative' applied voltage field assists deflection whilst a 'positive' applied voltage field inhibits deflection. An aluminium flap, with a Young's modulus of 70 GPa ($Z = 1.1$) can be assumed to have zero deflection, i.e. minimum mass transfer, for substrate thickness above 2 mm ($X = 4$). However, if the thickness of the flap is only 1.1 mm ($X = 2.2$) then the flap will be unable to 'close' within the substrate Young's Modulus range considered here.

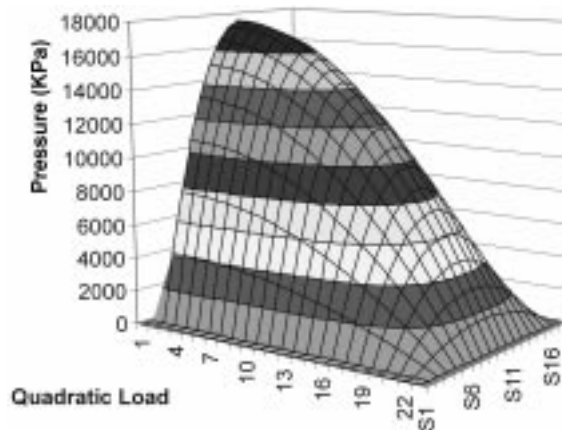


Fig. 10 Quadratic pressure loading

5.4 Quadratic pressure load predictions

The main advantage of FEM is that complex pressure loadings can be applied that reflect the real conditions more accurately, that is satisfy the boundary conditions. The basic boundary condition is that there is no pressure load at the flap edges. A parabolic load distribution was applied to the FE model with the numbering system used corresponding to the elements on the FE model (Fig. 10).

A maximum pressure of 17.64 kPa is used, which is the first order theoretical unimorph pressure difference. The pressure drops off to zero at the flap edges producing a more realistic loading and hence better deflection predictions. This loading cannot be implemented using the classical beam theory in which the pressure can be varied only along the length of the beam. No experimental data points could be obtained for deflection under for this pressure loading as all measuring techniques available are invasive and would alter the flow conditions being observed.

The tip deflections of the flap under the parabolic pressure distribution are plotted against the normalised substrate thickness (X) and the normalised substrate thickness (Z) (Figs. 11a & 11b). It is seen that as the substrate thickness and Young's Modulus are increased the tip deflection decreases. This is to be expected as the thicker and stiffer the substrate the more constrained the unimorph will be.

If the unimorph has to be capable of zero deflection to provide active control then, for a 500 V limit, the substrate has to be at least 0.9 mm thick ($X = 1.8$) for a 70 GPa Young's Modulus. Alternatively, a flap with a thickness of 1.1 mm requires a minimum Young's Modulus of only 50 GPa ($Z = 0.78$) for complete theoretical closure.

5.5 Piezoelectric limits

As stated earlier, piezoelectric materials have particular operating limits, for temperature, voltage and stress. The chemical composition of the material determines these limits. Operating outside these limits may cause partial or total depolarisation/breakdown of the material and a diminishing or loss of piezoelectric properties. This paper uses a limit of 500 V, which over the 0.5 mm piezoelectric ceramic equates an applied field of 1000 V/mm. Above this applied field the unimorph

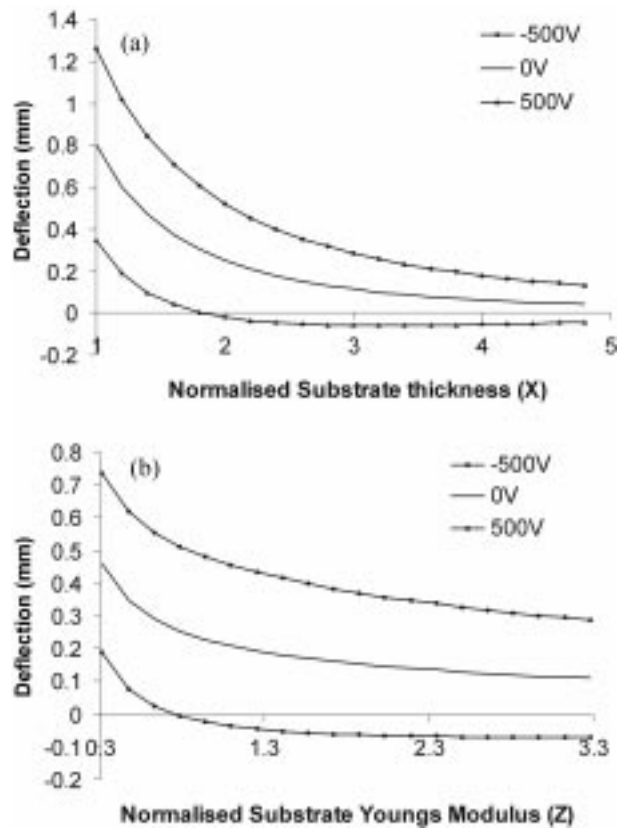


Fig. 11 FEM tip deflection predictions for a quadratic load for varying substrate: a) thickness; and b) Young's Modulus

was observed to breakdown. The nature of the breakdown is uncertain, possibly due to either the piezoelectric properties or the unimorph properties, i.e. arcing to the substrate.

FEM has the added advantage that the stresses due to the mechanical and electrical loads can be easily determined in each stage of deflection and in different configurations. It is suspected that breakdown occurs for an aluminium substrate (70 GPa) with thickness below 1.1 mm, due to the substantial load applied to piezoelectric ceramic from the acting pressure. This constrains the unimorph again and the design requires to be optimised for stress. However, the piezoelectric 'breakdown' characteristics of the material are still not fully determined.

6. Conclusions

The classical theory gives good correlation and accuracy with the FEM. FEM generally predicts greater deflection due to the support structure deflects and creates a non-zero slope at the start of the unimorph, which is not modelled by CPLT. The main disadvantage of the FEM over classical theory is its higher computational cost in terms of time and effort compared to the 'instant'

spreadsheet ability of the classical theory.

The design can be easily optimised to provide active control for substrate thickness and Young's Modulus. The thinner or more compliant the substrate the more mass transfer, deflection, can occur. Furthermore, zero deflection, for active control, limits the substrate to minimum thickness and stiffness. FEM gives the ability to analyse more complex pressure loadings that reflect the real boundary conditions. This enables improved FEM predictions of minimum thickness and stiffness over the classical theory.

The 'breakdown' characteristics seem to limit the unimorph design for stress and voltage levels. Another advantage of FEM is that stress levels in the unimorph can easily be obtained but more work is required to research the 'breakdown' characteristics of the piezoelectric material to provide an improved design analysis.

References

- Babinsky, H. (1999), "Control of swept shock wave/turbulent boundary-layer interactions", *ISSW22*. Imperial College, London, UK.
- Bahi, L., Ross, J.M. and Nagamatsu, H.T. (1983), "Passive shock wave/boundary layer control for transonic airfoil drag reduction", *AIAA 21st Aerospace Sciences Meeting*. Reno, USA.
- Chattopadhyay, A. and Seeley, C.E. (1997), "A higher order theory for modelling composite laminates with induced strain actuators", *Composites Part B*, **28B**, 243-252.
- Chen, C. *et al.* (1984), "Numerical study of porous airfoils in transonic flow", *AIAA J.*, **22**, 989-991.
- Couldrick, J.S. *et al.* (2001), "Swept shock wave boundary layer interaction control with "Smart" flap actuators", *Australian International Aerospace Conference*. Canberra, Australia.
- Couldrick, J.S. *et al.* (2002a), "Development of "Smart" flap actuators for swept shock wave boundary layer interaction control", *40th AIAA Aerospace Sciences Meeting & Exhibit*. Reno, USA.
- Couldrick, J.S. *et al.* (2002b), "Design optimisation of "Smart" flap actuators for swept shock wave boundary layer interaction control", *2nd Advances in Structural Engineering and Mechanics*. Pusan, Korea.
- Crawley, E.F. (1994), "Intelligent structures for aerospace: a technology overview and assessment", *AIAA J.*, **32**(8), 1689-1699.
- Crawley, E.F. and Luis, J. (1987), "Use of piezoelectric actuators as elements of intelligent structures", *AIAA J.*, **25**(10), October 1987, 1373-1385.
- Crawley, E.F. and Lazarus, K.B. (1991), "Induced strain actuation of isotropic and anisotropic plates", *AIAA J.*, **29**(6), 944-951.
- Delery, J.M. (1985), "Shock wave/turbulent boundary layer interaction and it's control", *Progress in Aerospace Science*, **22**, 209-228.
- Delery, J. and Bur, R. (1999), "Shock wave/boundary layer interaction and control techniques: a physical description", *ISSW22*. Imperial College, London, UK.
- Donthireddy, P. and Chandrashekhara, K. (1996), "Modeling and shape control of composite beams with embedded piezoelectric actuators", *Compos. Struct.*, **35**, 237-244.
- Gibson, R.F. (1994), *Principles of Composite Material Mechanics*, Sydney: McGraw-Hill.
- Gibson, T.M., Babinsky, H. and Squire, L.C. (2000), "Passive control of shock wave/boundary layer interactions", *Aeronautical J.*, 124-140.
- Hwang, W.-S. and Park, H.-C. (1993), "Finite element modeling of piezoelectric sensors and actuators", *AIAA J.*, **31**(5), 930-937.
- Krogmann, P., Stanewsky, E. and Thiede, P. (1985), "Effects of suction on shock/boundary-layer interaction and shock-induced separation", *J. Aircraft*, **22**(1), 37-42.
- Kubota, H. and Stollery, J.L. (1982), "An experimental study of the interaction between a glancing shock wave and a turbulent boundary layer", *J. Fluid Mech.*, **116**, 431-458.
- Matthew, J., Sankar, B. and Cattafesta, L. (2001), "Finite element modelling of piezoelectric actuators for active

- flow control applications", *39th AIAA Aerospace Sciences Meeting and Exhibit*. Reno, Nevada, USA.
- Mukherjee, A. and Joshi, S. (2002), "Piezoelectric sensor and actuator spatial design for shape control of piezolaminated plates", *AIAA J.*, **40**(6), 1204-1210.
- Nagamatsu, H.T., Ficarra, R.V. and Dyer, R. (1985), "Supercritical airfoil drag reduction by passive shock wave/boundary layer control in the mach number range .75 to .90", *AIAA 23rd Aerospace Sciences Meeting*. Reno, Nevada, USA.
- Nagamatsu, H.T., Mitty, T.J. and Nyberg, G.A. (1987), "Passive shock wave/boundary layer control of a helicopter rotor airfoil in a contoured transonic wind tunnel", *AIAA 25th Aerospace Sciences Meeting*. Reno, Nevada, USA.
- Raghunathan, S. (1987), "Effects of porosity strength on passive shock-wave/boundary layer control", *AIAA J.*, **25**(5), 757-758.
- Raghunathan, S. and Mabey, D.G. (1987), "Passive shock-wave/boundary layer control on a wall-mounted model", *AIAA J.*, **25**(2), 275-278.
- Raghunathan, S., Gray, J.L. and Cooper, R.K. (1987), "Effects of inclination of holes on passive shock wave boundary layer control", *AIAA 25th Aerospace Sciences Meeting*. Reno, Nevada, USA.
- Raghunathan, S. (1988), "Passive control of shock-boundary layer interaction", *Progress in Aerospace Science*, **25**, 271-296.
- Savu, G. and Trifu, O. (1984), "Porous airfoils in transonic flow", *AIAA J.*, **22**(7 - Technical Notes): 989-991.
- Soares, C.M.M., Soares, C.A.M. and Correia, V.M.F. (1999), "Optimal design of piezolaminated structures", *Compos. Struct.*, **47**, 625-634.
- Vel, S.S. and Batra, R.C. (2000), "Cylindrical bending of laminated plates with distributed and segmented piezoelectric actuators/sensors", *AIAA J.*, **38**(5), 857-867.
- Yam, L.H. and Yan, Y.J. (2002), "Optimal design of thickness and embedded depth of piezoelectric actuator in piezo-laminated structures", *2nd Advances in Structural Engineering and Mechanics*. Pusan, Korea.